# Interplay between Edge-to-Face Aromatic and Hydrogen-Bonding Interactions

**Daniel Escudero, Antonio Frontera,* David Quiñonero,* and Pere M. Deyà**

*Departament de Química, Universitat de les Illes Balears, 07122 Palma de Mallorca, Spain*

*Received: March 18, 2008; Revised Manuscript Received: April 22, 2008*

The interplay between two important noncovalent interactions involving aromatic rings is studied by means of MP2/6-31++G** ab initio calculations. They indicate that synergistic effects are present in complexes where edge-to-face aromatic interactions and hydrogen-bonding interactions coexist. These synergistic effects have been studied bu using the atoms in molecules theory and the molecular interaction potential with polarization partition scheme. Experimental evidence for such interactions has been obtained from the Cambridge Structural Database.

## Introduction

Noncovalent interactions involving aromatic rings are key processes in both chemical and biological recognition,[1] because supramolecular chemistry relies on these forces. Interactions between aromatic rings ($\pi-\pi$ interactions) contribute to protein and DNA stability[2] and form recognition motifs in proteins and enzymes.[3] Several studies suggest the existence of a competition between stacking and T-shaped (edge-to-face) $\pi-\pi$ complexes involving aromatic amino acids. This competition[4] is strongly affected by the polarity of the environment and by the possibility of forming hydrogen bonds.[5] The latter point is still under discussion, because recent studies have shown (i) that the favorable nature of stacked conformations in protein environment must not be related with the higher accessibility of H-bond forming groups[6] and (ii) that the $\pi-\pi$ interaction on itself does not have an overall strengthening on hydrogen bonding in DNA.[7]

The $\pi-\pi$ interaction is dominated by dispersion and electrostatic (quadrupole−quadrupole) forces. The T-shape orientation has favorable electrostatics but weaker dispersion, and it is very close in energy to the parallel displaced configuration that has more dispersion but less favorable electrostatics. High accuracy benchmark calculations on the benzene dimer (QCISD(T)/aug-cc-pVTZ level of theory) demonstrate that both configurations have a binding energy of 10.45 kJ/mol.[8] This result is in line with the competition between stacking and T-shape configurations in $\pi-\pi$ aromatic interactions in amino acids.[4a] The hydrogen-bond interaction is mainly dominated by electrostatic effects (dipole−dipole interactions).[9]

We have recently reported experimental[10] and theoretical[11] evidence of interesting synergistic effects between anion$-\pi$[12] and $\pi-\pi$ interactions. We have demonstrated that there is a remarkable interplay between the anion$-\pi$ and $\pi-\pi$ interactions in complexes where both interactions coexist. This interplay can lead to strong cooperative effects, as has been recently demonstrated in nitrate−triazine−triazine complexes.[13] Moreover, we have also demonstrated synergistic effects between C−H/$\pi$ and $\pi-\pi$ interactions by means of ab initio calculations, and experimental evidence was obtained from the Protein Data Bank.[14] In the present report, we study how the T-shape $\pi-\pi$ interaction is influenced if the arene participates in hydrogen-bonding interactions. Previous works have studied the influence of stacking on hydrogen bonding.[7,15] However, to the best of our knowledge, this is the first study that deals with the interplay between the T-shape $\pi-\pi$ and hydrogen-bonding interactions. We have selected three aromatic rings, that is, **3**−**5** (Figure 1), that contain nitrogen atoms in the structure which can participate in hydrogen-bonding interactions ($\sigma$ interactions). We have first computed the hydrogen-bonded and $\pi-\pi$ complexes **6**−**17** depicted in Figures 1 and 2. Because the aromatic rings **3** (pyridine) and **4** (pyridazine) can act as hydrogen-bond acceptors and the pyrrole **5** can act as hydrogen-bond donor, we have computed the $\pi-\pi-\sigma_{acceptor}$ complexes **18**−**25** and the $\pi-\pi-\sigma_{donor}$ complexes **26**−**29** represented in Figure 3, in order to study the interplay between the $\pi-\pi$ and hydrogen-bonding interactions. Moreover, we have also studied the effect of using an electron-deficient aromatic ring (hexafluorobenzene instead of benzene) on the stability of the T-shape $\pi-\pi$ complexes and

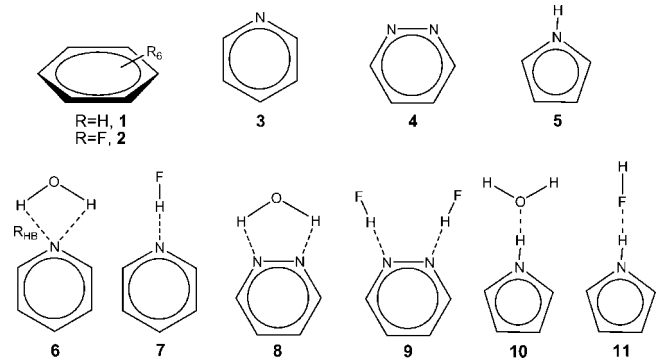


**Figure 1.** Schematic representation of compounds **1**−**5** and H-bonded complexes **6**−**11**.

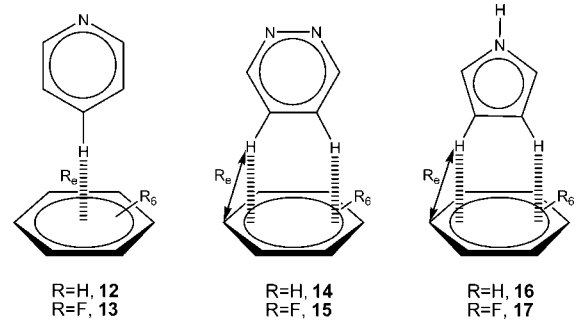


**Figure 2.** Schematic representation of binary complexes **12**−**17**.

* Corresponding author. E-mail: toni.frontera@uib.es.

10.1021/jp802370s CCC: $40.75 © 2008 American Chemical Society
Published on Web 06/11/2008

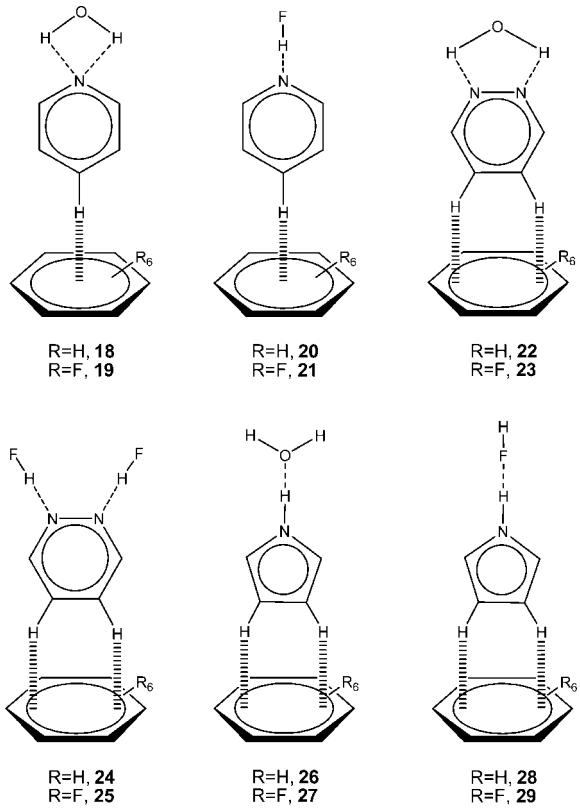


**Figure 3.** Schematic representation of ternary complexes and quaternary complexes **18**−**29**.

the influence on the interplay between the $\pi-\pi$ and hydrogen-bonding interactions. We have used the Bader's theory of atoms in molecules (AIM),[16] which has been widely used to characterize a great variety of interactions,[17] to analyze cooperative effects in the complexes.

## Theoretical Methods

The geometries of all complexes studied in this work were fully optimized at the MP2/6-31++G** level of theory by using the Gaussian03 program.[18] The binding energies were calculated with correction for the basis set superposition error (BSSE) by using the Boys−Bernardi counterpoise technique.[19] The optimization of the complexes has been performedby imposing $C_{2v}$ symmetry. Other possible conformations of complexes have not been considered because the ultimate aim of this study is to verify the interplay between both noncovalent interactions in the ternary systems and to obtain an insight into the nature of the cooperativity. Therefore, we have concentrated only on those complex geometries. A possible disadvantage of imposing symmetry is that highly nonsymmetrical conformations may often have similar or even higher binding energy compared to those of the more symmetric ones.[20] In spite of this possible drawback due to the imposed $C_{2v}$ symmetry, it is likely that the trends of the results discussed in this article will remain valid.

It is known that the MP2 level tends to overestimate the binding energy of the three main conformations of the benzene dimer compared to higher levels of theory.[8] It should be also mentioned that the T-shape geometry is the conformation where the agreement between MP2 and QCISD(T)/aug-cc-pVQZ levels of theory is better. Moreover, the main objective of this study is not to obtain the highest accuracy for each binding energy. Instead, it is, as aforementioned, to obtain an insight into the interplay between both noncovalent interactions studied in this work.

**TABLE 1: Binding Energies without and with the BSSE Correction, ($E$ and $E_{BSSE}$, kJ/mol, respectively) and Equilibrium Distances for the Hydrogen-Bonding and T-Shape Interactions ($R_{HB}$ and $R_e$, Å, respectively) at MP2/6-31++G** Level of Theory for Complexes 6−17**

| complex | $E$ | $E_{BSSE}$ | $R_{HB}$ or $R_e$ |
|---|---|---|---|
| **6** (**3** + $H_2O$) | −16.59 | −11.29 | 2.723 |
| **7** (**3** + HF) | −58.81 | −50.24 | 1.644 |
| **8** (**4** + $H_2O$) | −30.60 | −23.78 | 2.376 |
| **9** (**4** + 2HF) | −100.19 | −84.39 | 1.733 |
| **10** (**5** + $H_2O$) | −29.76 | −21.19 | 1.962 |
| **11** (**5** + HF) | −13.25 | −10.37 | 2.121 |
| **12** (**1** + **3**) | −23.12 | −7.98 | 2.304 |
| **13** (**2** + **3**) | −15.88 | −0.46 | 2.373 |
| **14** (**1** + **4**) | −21.78 | −10.41 | 2.783[a] |
| **15** (**2** + **4**) | −13.13 | 0.04 | 2.805[a] |
| **16** (**1** + **5**) | −14.76 | −4.60 | 2.879[a] |
| **17** (**2** + **5**) | −19.14 | −5.77 | 2.763[a] |

[a] $R_e$ is measured from the hydrogen atom to the nearest carbon atom of the benzene/hexafluorobenzene.

The AIM analysis has been performed by means of the AIM2000 version 2.0 program[21] by using the MP2/6-31++G** wavefunction. The physical nature of the noncovalent interactions has been studied by using the molecular interaction potential with polarization (MIPp)[22] method. The MIPp is a convenient tool for predicting binding properties. It has been successfully used for rationalizing molecular interactions such as hydrogen-bonding and ion$-\pi$ interactions and for predicting molecular reactivity.[23] The MIPp partition scheme is an improved generalization of the molecular electrostatic potential (MEP), where three terms contribute to the interaction energy: (i) an electrostatic term identical to that of the MEP,[24] (ii) a classical dispersion−repulsion term,[25] and (iii) a polarization term derived from perturbational theory.[26]

## Results and Discussion

**Energetic and Geometrical Details.** In Table 1, we summarize the binding energies without and with the BSSE correction ($E$ and $E_{BSSE}$, respectively) and equilibrium distances ($R_{HB}$ and $R_e$) of complexes **6**−**14** at the MP2/6-31++G** level of theory. The energetic features of the hydrogen-bonded complexes **6**−**11** depend upon the model molecule used as hydrogen-bond acceptor/donor. In complexes **7** and **9** (HF, hydrogen-bond donor), each hydrogen bond has an interaction energy of approximately −40 kJ/mol, considerably more negative than those obtained for complexes **6** and **8** ($H_2O$, hydrogen-bond donor). Conversely, the binding energy computed for the interaction of pyrrole with water (complex **10**) is more favorable than the one of pyrrole with HF (complex **11**), indicating that $H_2O$ is a better hydrogen-bond acceptor than HF. The binding energies computed for the T-shape complexes of compounds **3**−**5** with benzene (**12**, **14**, and **16**) are negative, indicating a favorable interaction. In contrast, the binding energies computed for the T-shape complexes of compounds **3** and **4** with hexafluorobenzene ($\pi_F$) are negligible, indicating that the edge-to-face $\pi-\pi_F$ interaction with an electron-deficient ring is disfavored in comparison with the standard $\pi-\pi$ interaction. Conversely, for complex **17** (pyrrole−hexafluorobenzene), the interaction is favorable and, surprisingly, more favorable than the interaction with benzene (see Table 1). A likely explanation is that the geometrical characteristic of the five-membered ring allows the hydrogen atoms of pyrrole to interact with the fluorine atoms of the HFB.

The geometric and energetic results computed for the complexes **18**−**29** are summarized in Table 2. Some very

**TABLE 2: Binding, Synergistic, and Non-additivity Energies with BSSE Correction ($E_{BSSE}$, $E_{syn}$, and $E - E_A$, kJ/mol, respectively), Equilibrium Distances ($R_e$ and $R_{HB}$, Å) at the MP2/6-31++G** Level of Theory**

| complex | $E$ | $E_{BSSE}$ | $E_{syn}$ | $E - E_A$ | $R_e$ | $R_{HB}$ | $\Delta R_e$ | $\Delta R_{HB}$ |
|---|---|---|---|---|---|---|---|---|
| **18** | −41.13 | −20.19 | −0.92 | −2.38 | 2.291 | 2.722 | −0.013 | −0.001 |
| **19** | −31.98 | −10.95 | 0.75 | −1.38 | 2.370 | 2.744 | −0.003 | +0.021 |
| **20** | −84.35 | −60.28 | −2.05 | −7.73 | 2.291 | 1.635 | −0.013 | −0.009 |
| **21** | −73.07 | −49.07 | 1.63 | −4.35 | 2.373 | 1.652 | +0.000 | +0.008 |
| **22** | −54.17 | −35.49 | −1.25 | −2.93 | 2.764[a] | 2.367 | −0.019 | −0.009 |
| **23** | −43.05 | −22.70 | 1.05 | −1.34 | 2.803[a] | 2.386 | −0.002 | +0.010 |
| **24** | −127.36 | −98.77 | −4.01 | −12.67 | 2.726[a] | 1.722 | −0.037 | −0.011 |
| **25** | −110.98 | −81.55 | 2.76 | −6.73 | 2.806[a] | 1.740 | +0.001 | +0.007 |
| **26** | −43.68 | −24.87 | 0.92 | −0.21 | 2.883[a] | 1.968 | +0.004 | +0.006 |
| **27** | −50.91 | −28.30 | −1.34 | −2.38 | 2.737[a] | 1.950 | −0.026 | −0.012 |
| **28** | −27.50 | −14.34 | 0.59 | −0.25 | 2.884[a] | 2.123 | +0.005 | +0.002 |
| **29** | −33.61 | −16.89 | −0.71 | −1.67 | 2.741[a] | 2.099 | −0.022 | −0.022 |

[a] $R_e$ is measured from the hydrogen atom to the nearest carbon atom of the benzene/hexafluorobenzene, see Figure 2.

interesting points can be extracted from the geometrical results. The equilibrium distance ($R_e$) of the T-shape interaction in the $\pi-\pi-\sigma_{acceptor}$ complexes **18**, **20**, **22**, and **24** shortens when compared to that of binary complexes **12** and **14**, indicating that the presence of the $\sigma$ interaction strengthens the $\pi-\pi$ interaction. In addition, the equilibrium distance of the $\sigma$ interaction ($R_{HB}$) also shortens with respect to that of the hydrogen-bonding complexes **6**−**9**, indicating that the presence of the $\pi-\pi$ interaction strengthens the hydrogen-bond interaction. An opposite behavior is observed in the $\pi_F-\pi-\sigma_{acceptor}$ ternary complexes **21** and **25**, where an elongation of both distances is observed, indicating that both hydrogen-bonding and $\pi_F-\pi$ interactions are weakened. For pyridine and pyridazine, $\pi_F-\pi-\sigma_{acceptor}$ complexes **19** and **23**, a reverse behavior of both interactions is observed. For both complexes, an elongation of the hydrogen-bond interaction and a shortening of the $\pi_F-\pi$ interaction is observed, indicating that in these complexes, the $\pi_F-\pi$ noncovalent interaction increases at the expense of the hydrogen-bond interaction, which diminishes. Finally, the equilibrium distance ($R_e$) of the T-shape interaction in the $\pi-\pi-\sigma_{donor}$ ternary complexes **26** and **28** lengthens when compared to that of the binary complex **16**, indicating that the presence of the $\sigma$ interaction weakens the $\pi-\pi$ interaction. In addition, the equilibrium distance of the $\sigma$ interaction ($R_{HB}$) in complexes **26** and **28** also lengthens with respect to that of the hydrogen-bonding complexes **10** and **11**, respectively, indicating that the presence of the $\pi-\pi$ interaction weakens the hydrogen-bond interaction. An opposite behavior is observed in the $\pi_F-\pi-\sigma_{donor}$ ternary complexes **27** and **29**, where a shortening of both distances is observed, indicating that both hydrogen-bonding and $\pi-\pi_F$ interactions are strengthened.

We have included in Table 2 what we entitle synergistic energies ($E_{syn}$), which is the difference between the binding energy (BSSE corrected) of the complexes **18**−**29** and the binding energy of the related hydrogen-bonding (**6**−**11**) and $\pi-\pi$ (**12**−**17**) complexes. For instance, in complex **18** (**1**···**3**···HF), we have computed the synergistic energy by subtracting the interaction energies of **3**···HF (complex **7**) and **1**···**3** (complex **12**) from the binding energy of **18**. This value gives valuable information regarding the interplay between both noncovalent interactions present in the complexes. It is worth mentioning that this term is negative in the complexes **18**, **20**, **22**, **24**, **27**, and **29**, in agreement with the shortening of the equilibrium distances $R_e$ and $R_{HB}$, indicating that both interactions strengthen. In contrast, in the complexes **21**, **25**, **26**, and **28**, the synergistic energy is positive, in agreement with the lengthening of the equilibrium distances $R_e$ and $R_{HB}$, indicating that both interactions weaken. As aforementioned, in $\pi_F-\pi-\sigma_{acceptor}$ complexes **19** and **23**, one noncovalent interaction enhances at the expense of the other. The synergistic energy is positive in both complexes, where the hydrogen-bond lengthens and the $\pi-\pi_F$ shortens, indicating that, in these complexes, the stronger interaction (hydrogen bonding) has more weight and dominates the synergy. We have also studied the mutual influence between both interactions by computing the genuine non-additivity energies for complexes **18**−**29**, which are summarized in Table 2. The non-additivity energy ($E - E_A$) is the difference between the binding energy of the complex and the binding energy of the sum of all pair interaction energies (denoted as $E_A$). For instance, in complex **19** (**1**···**3**···HF), we have computed the non-additivity energy by subtracting the sum of three pair interaction energies, (i) **1**···**3**, (ii) **3**···HF, and (iii) **1**···HF, from the binding energy of **19**. It is worth mentioning that this term is negative in all complexes, in disagreement with the $E_{syn}$ energies and the geometrical analysis. In order to shed light into this discordant results, we have used two additional criteria to analyze the mutual influence of both interactions in the ternary complexes, that is, the AIM and MIPp methods, as discussed further on.

**AIM Analysis.** The AIM analysis is summarized in Table 3 and gives some helpful information regarding the strength of the noncovalent interactions involved in the complexes. It has been demonstrated that the value of the electron charge density at the critical points (CPs) that are generated in $\pi-\pi$ and hydrogen-bonded complexes can be used as a measure of the bond order.[17,27] In Figure 4, we show the distribution of CPs in complexes **18**, **20, 22, 24, 26**, and **21**, where benzene is involved. The distribution is identical to those obtained for hexafluorobenzene complexes, which is shown in the Supporting Information (Figure S1). In complexes **18**−**21** (pyridine complexes), six bond CP, six ring CPs, and one cage CP describe the edge-to-face $\pi-\pi$ interaction. The bond CPs connect the hydrogen atom with the carbon atoms of the ring, and the ring CPs connect the hydrogen atom with the middle of the C−C bonds. The cage CP connects the hydrogen atom with the middle of the aromatic ring. The hydrogen-bond interaction is described by one bond CP, see Figure 4. In complexes **22**−**29** (pyridazine and pyrrole complexes), two bond CPs, two ring CPs, and one cage CP describe the edge-to-face $\pi-\pi$ interaction. The bond CPs connect two hydrogen atoms with two carbon atoms of the ring, and the ring CPs connect two hydrogen atoms with the middle of two C−C bonds. The cage CP connects the hydrogen atom with the middle of the aromatic ring. The hydrogen-bond interaction is described by two bond CPs and one ring CP if the hydrogen-bond donor is water in pyridazine complexes (**22** and **23**), and it is described by one bond CP in

**TABLE 3: Electron Charge Density ($\rho$, au) and its Laplacian ($\nabla^2\rho$, au) Computed at the Bond and Cage ($\pi-\pi$) CP for complexes 4−21 and Variation of the Charge Density ($\Delta\rho$) upon Formation of the Ternary and Quaternary Complexes 14−21[a]**

| complex | I | $\rho \times 10^2$ | $\nabla^2\rho \times 10$ | $\Delta\rho \times 10^3$ | $\Delta R_e/\Delta R_{HB}$ |
|---|---|---|---|---|---|
| **18** | $\pi-\pi$ | 0.6750 | 0.3259 | 0.121 | −0.013 |
| (**1**···**3**···$H_2O$) | HB | 0.7777 | 0.3047 | 0.042 | −0.001 |
| **19** | $\pi-\pi$ | 0.6165 | 0.2875 | 0.019 | −0.003 |
| (**2**···**3**···$H_2O$) | HB | 0.7408 | 0.2902 | −0.328 | +0.021 |
| **20** | $\pi-\pi$ | 0.6741 | 0.3248 | 0.112 | −0.013 |
| (**1**···**3**···HF) | HB | 5.5672 | 1.3487 | 1.492 | −0.009 |
| **21** | $\pi-\pi$ | 0.6132 | 0.2850 | −0.014 | 0.000 |
| (**2**···**3**···HF) | HB | 5.2930 | 1.3599 | −1.249 | +0.008 |
| **22** | $\pi-\pi$ | 0.1985 | 0.0997 | 0.054 | −0.019 |
| (**1**···**4**···$H_2O$) | HB | 1.1940 | 0.4293 | 0.232 | −0.009 |
| **23** | $\pi-\pi$ | 0.1890 | 0.0922 | 0.007 | −0.002 |
| (**2**···**4**···$H_2O$) | HB | 1.1445 | 0.4155 | −0.264 | +0.010 |
| **24** | $\pi-\pi$ | 0.2097 | 0.1049 | 0.166 | −0.037 |
| (**1**···**4**···2HF) | HB | 4.3486 | 1.3279 | 1.293 | −0.011 |
| **25** | $\pi-\pi$ | 0.1874 | 0.0914 | −0.009 | +0.001 |
| (**2**···**4**···2HF) | HB | 4.1359 | 1.3012 | −0.834 | +0.007 |
| **26** | $\pi-\pi$ | 0.1644 | 0.0835 | −0.008 | +0.004 |
| (**1**···**5**···$H_2O$) | HB | 2.1152 | 0.7505 | −0.290 | +0.006 |
| **27** | $\pi-\pi$ | 0.2112 | 0.1015 | 0.089 | −0.026 |
| (**2**···**5**···$H_2O$) | HB | 2.1977 | 0.7838 | 0.534 | −0.012 |
| **28** | $\pi-\pi$ | 0.1640 | 0.0833 | −0.013 | +0.005 |
| (**1**···**5**···HF) | HB | 1.1172 | 0.4989 | −0.055 | +0.002 |
| **29** | $\pi-\pi$ | 0.2096 | 0.1008 | 0.073 | −0.022 |
| (**2**···**5**···HF) | HB | 1.1817 | 0.5222 | 0.590 | −0.022 |

[a] I, interaction; HB, hydrogen-bond; $\pi-\pi$, edge-to-face stacking.

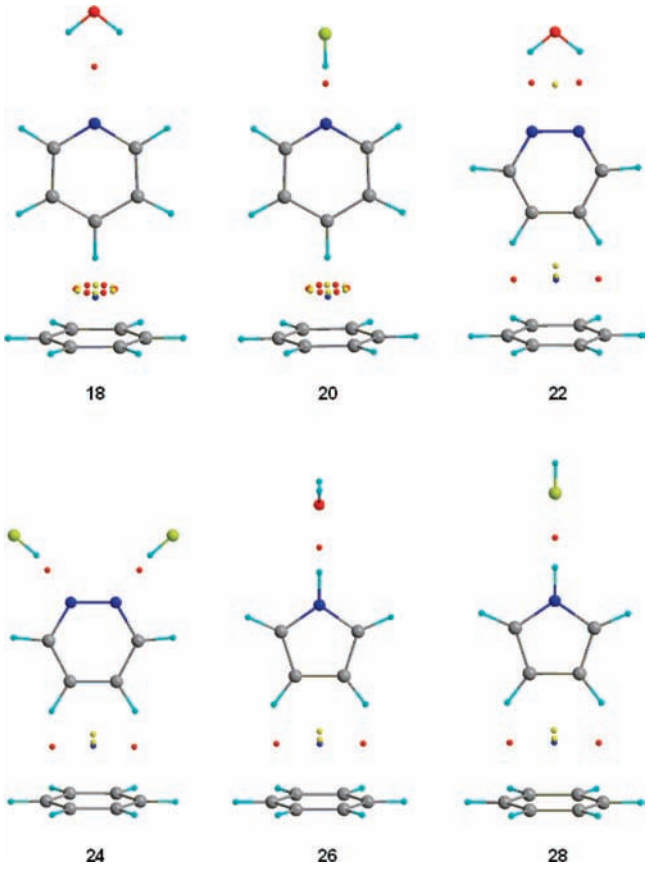


**Figure 4.** Schematic representation of the location of bond (red), ring (yellow), and cage (blue) CPs in complexes **18**, **20**, **22**, **24**, **26**, and **28**.

the rest of the complexes (**24**−**29**), see Figure 4. In Table 3, we show the values of the electron charge density ($\rho$) and its Laplacian ($\nabla^2\rho$) computed at the cage and bond CP that characterize the $\pi-\pi$ interaction and hydrogen-bonding interaction, respectively. We also summarize the variation of the $\rho$ value in complexes **18**−**29** (both interactions coexist) with respect to complexes **6**−**17** (only one interaction is present). These values give information about the interplay between the noncovalent interaction involved in the complexes. The values obtained for the Laplacian are in all cases positive, as is common in closed-shell interactions. First, it is worth mentioning that the value of the charge density computed at the bond and cage CPs is greater in complexes **18, 20, 22, 24, 27**, and **29** than in complexes **3**−**17**, in agreement with the computed synergistic energies and confirming that the coexistence of $\pi-\pi$ and hydrogen-bonding interactions in these complexes involves a strengthening of both. Second, the value of the charge density computed at the bond and cage CPs is smaller in complexes **21**, **25**−**26**, and **28** than in complexes **3**−**17**, in agreement with the positive values obtained for synergistic energy and with the lengthening of equilibrium distances, indicating that both interactions weaken. It should be mentioned that these results are in disagreement with the non-additivity energies, which are in all complexes negative. Third, in complexes **19** and **23**, the variation ($\Delta\rho$) of the charge density at the cage CP ($\pi-\pi$ interaction) is positive, indicating that the $\pi-\pi$ interaction strengthens, and the variation at the bond CP (hydrogen-bond interaction) is negative, indicating a reduction of the interaction. It can be observed that the variation of $\rho$ is, in absolute value, more important in the bond CP, indicating that the hydrogen-bond interaction is weakened more than the $\pi-\pi$ interaction is strengthened, which explains the positive synergistic energy.

**TABLE 4: Contributions to the Total ($E_t$) Interaction Energy (kJ/mol) Computed by Using MIPp of Compounds 3−5 and 12−17 Interacting with $H^{1/4+}$ or $O^{1/2-}$ at the Minimum along the Line Defined by the Ideal Interacting Trajectory for a Hydrogen Bond**

| complex | $E_e$ | $E_p$ | $E_{vw}$ | $E_t$ |
|---|---|---|---|---|
| **3** + $H^{\bullet+}$ | −46.90 | −6.77 | 6.52 | −47.15 |
| **4** + $H^{\bullet+}$ | −44.85 | −6.19 | 4.77 | −46.27 |
| **5** + $O^{1/2-}$ | −48.78 | −8.03 | 5.64 | −51.16 |
| **12** + $H^{\bullet+}$ | −49.87 | −6.35 | 5.85 | −50.37 |
| **13** + $H^{\bullet+}$ | −43.35 | −6.60 | 5.14 | −44.81 |
| **14** + $H^{\bullet+}$ | −47.78 | −6.06 | 3.89 | −49.95 |
| **15** + $H^{\bullet+}$ | −43.10 | −6.44 | 5.52 | −44.02 |
| **16** + $O^{1/2-}$ | −43.56 | −7.94 | 4.05 | −47.44 |
| **17** + $O^{1/2-}$ | −54.93 | −8.61 | 7.65 | −55.89 |

**MIPp Analysis.** Finally, we have used the MIPp partition scheme to analyze the physical nature of the hydrogen-bond interaction involved in the complexes and to understand the bonding mechanism and the synergistic energies. We have computed the MIPp of compounds **3**−**5, 12**−**17** interacting with either $H^{1/4+}$ (pyridine and pyridazine $\sigma_{acceptor}$ complexes) or $O^{1/2-}$ (pyrrole $\sigma_{donor}$ complexes) in order to analyze the hydrogen-bonding interaction in the absence (**3**−**5**) and presence (**12**−**17**) of $\pi-\pi$ interaction (see Table 4). In compounds **3**−**5**, the total interaction ($E_t$) is basically dominated by electrostatic effects ($E_e$), because the polarization ($E_p$) and dispersion−repulsion ($E_{vw}$) contributions are small. In compounds **12** and **14** interacting with $H^{1/4+}$ (favorable synergism), the $E_e$ term becomes more negative, and the $E_p$ term remains almost constant, in comparison with those in compounds **3**−**4**, indicating that the synergism is due to electrostatic effects. A similar behavior is found for compound **17** interacting with $O^{1/2-}$ (favorable synergism). In contrast, in compounds **13** and **15** interacting with $H^{1/4+}$, the $E_e$ term turns out to be more positive, and the $E_p$ remains almost

constant, with respect to those in compounds **3**−**5** interacting with $H^{1/4+}$, indicating that the unfavorable synergism of these complexes is due to a diminution of the electrostatic interaction when the arene participates in $\pi-\pi_F$ interactions. The same behavior is found for **16** interacting with $O^{1/2-}$ (unfavorable synergism). In this case, when the arene participates in $\pi-\pi$ interaction, the hydrogen-bond donor capacity of pyrrole is diminished.

The MIPp analysis is in accord with the AIM results, the synergistic energies ($E_{syn}$), and the geometrical features of the complexes ($\Delta R_e$ and $\Delta R_{HB}$ parameters). The non-additivity energies disagree with the aforementioned criteria. Consequently, the evaluation of the mutual influence of hydrogen-bonding and T-shape $\pi-\pi$ noncovalent interactions by using genuine non-additivity energies is not recommended, at least in the systems studied here. A likely explanation is that the additivity energy of all hypothetical dimers is computed by using the geometry of the complex where both interactions coexist. Therefore, in systems where the mutual influence of both noncovalent interactions has an important effect on the equilibrium distances, each pair T-shape/$\pi-\pi$ and $\pi-\sigma_{donor/acceptor}$ is far from the ground-state geometry, and consequently, the $E_A$ term is influenced by this issue.

**Cambridge Structural Database Search.** In order to obtain experimental evidence of the possible coexistence of both hydrogen-bond and T-shape $\pi-\pi$ interactions in the solid state, we have performed a search in the Cambridge Structural Database (CSD).[28] Crystal structures are so rich in geometrical information and often reveal effects that have not been noticed by the original authors. The utility of crystallography and the CSD in analyzing geometrical parameters and noncovalent interactions is clearly established.[29] In exploring the CSD for pyridine simultaneously interacting with a hydrogen-bond donor and establishing an edge-to-face $\pi-\pi$ interaction, we have found 45 fragments that correspond to 22 structures (listed in the Supporting Information). The search has been performed by imposing several constraints. First, a hit is stored when six nonbonded contacts exist between the aromatic hydrogen atom of the pyridine and the six carbon atoms of the aromatic ring. Second, a hit is stored if the nitrogen atom of the pyridine is participating in conventional hydrogen bonding (unconventional C−H···N hydrogen bonds have not been considered). Third, to ensure the T-shape geometry, we have constrained the angle between the pyridine and phenyl ring planes to range between 150 and 210°. Fourth, only organic compounds have been explored, because the binding ability of the aromatic rings belonging to organometallic complexes can be influenced by the metal. In Figure 5, we show two examples (CSD codes FEPBOS[30] and MAFQIU[31]) where the combination of both interactions determines the crystal packing. It is worth mentioning that a similar search performed for pyrrole, which has unfavorable hydrogen-bond/$\pi-\pi$ synergy, has not revealed any hit. Because of the reduced number of pentafluorophenyl derivatives present in the CSD (only organics), the searches for the coexistence of $\pi_F-\pi-\sigma_{donor}$ interactions (favorable synergism) are not relevant. The same line of reasoning is applicable to pyridazine derivatives.

## Concluding Remarks

In summary, the results reported in this manuscript stress the importance of noncovalent interactions involving aromatic systems and the interplay among them that can lead to synergistic effects (up to 7% of the total interaction energy). Because of the presence of a great number of aromatic rings containing hetero-atoms in biological systems, this effect can be important and might help understand some biological processes where the interplay between both interactions exist. It also should be taken into account in supramolecular chemistry and crystal engineering fields.

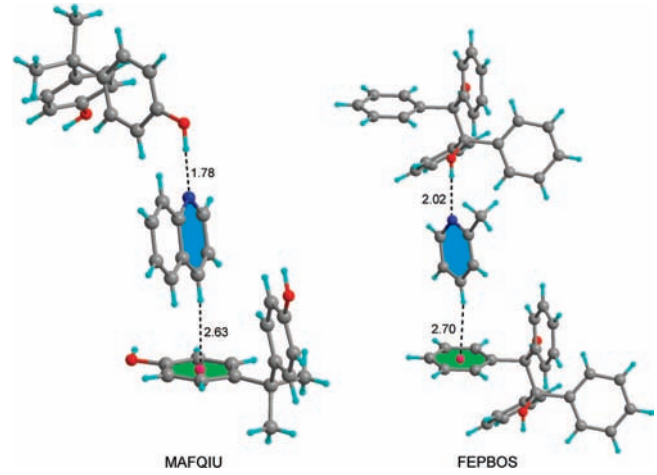


**Figure 5.** Partial views of the x-ray structures corresponding to 4,4′-isopropylidenebisphenol quinoline clathrate (MAFQIU) and 1,1,2,2-tetraphenylethan-1,2-diol *bis*(2-picoline) clathrate (FEPBOS).

**Acknowledgment.** We thank the DGICYT of Spain and Govern Balear (Projects CTQ2005-08989-01 and PROGECIB-33A, respectively) for financial support. We thank the Centre de Supercomputació de Catalunya (CESCA) for computational facilities. D.E. thanks Fundació Sa Nostra for a fellowship.

**Supporting Information Available:** The Supporting Information for this paper includes the cartesian coordinates of MP2/6-31++G** optimized structures and complexes **3**−**29**, the representation of the CP in complexes **19**, **21**, **23**, **25**, **27**, and **29**, and the list of the CSD reference codes of the x-ray structures. This material is available free of charge via the Internet at http://pubs.acs.org.

## References and Notes

(1) Meyer, E. A.; Castellano, R. K.; Diederich, F. *Angew. Chem., Int. Ed.* **2003**, *42*, 1210.

(2) (a) Burley, S. K.; Petsko, G. A. *Science* **1985**, *229*, 23. (b) Hunter, C. A.; Sanders, J. K. M. *J. Am. Chem. Soc.* **1990**, *112*, 5525. (c) Chakrabarti, P.; Samanta, U. *J. Mol. Biol.* **1995**, *251*, 9.

(3) (a) Samanta, U.; Chakrabarti, P. *Protein Eng.* **2001**, *14*, 7. (b) Macias, M.; Wiesner, S.; Sudol, M. *FEBS Lett.* **2002**, *513*, 30.

(4) (a) Chelli, R.; Gervasio, F. L.; Procacci, P.; Schettino, V. *J. Am. Chem. Soc.* **2002**, *124*, 6133. (b) Meurisse, R.; Brausseur, R.; Thomas, A. *Biochim. Biophys. Acta* **2003**, *1649*, 86.

(5) Mitchell, J. B.; Nandi, C. L.; McDonald, I. K.; Thornton, J. M.; Price, S. L. *J. Mol. Biol.* **1994**, *239*, 315.

(6) Cauët, E.; Rooman, M.; Wintjens, R.; Liévin, J.; Biot, C. *J. Chem. Theor. Comput.* **2005**, *1*, 472.

(7) Vanommeslaeghe, K.; Mignon, P.; Loverix, S.; Tourwé, D.; Geerlings, P. *J. Chem. Theor. Comput.* **2006**, *2*, 1444.

(8) Janowski, T.; Pulay, P. *Chem. Phys. Lett.* **2007**, *447*, 27, and references cited therein.

(9) Jeffrey. G. A. *An Introduction to Hydrogen Bonding (Topics in Physical Chemistry)*; Oxford University Press: New York, 1997.

(10) Garcia-Raso, A.; Alberti, F. M.; Fiol, J. J.; Tasada, A.; Barceló-Oliver, M.; Molins, E.; Escudero, D.; Frontera, A.; Quiñonero, D.; Deyà, P. M. *Inorg. Chem.* **2007**, *46*, 10724.

(11) (a) Frontera, A.; Quiñonero, D.; Costa, A.; Ballester, P.; Deyà, P. M. *New J. Chem.* **2007**, *31*, 556. (b) Quiñonero, D.; Frontera, A.; Garau, C.; Ballester, P.; Costa, A.; Deyà, P. M. *ChemPhysChem* **2006**, *7*, 2487.

(12) Quiñonero, D.; Garau, C.; Rotger, C.; Frontera, A.; Ballester, P.; Costa, A.; Deyà, P. M. *Angew. Chem., Int. Ed.* **2002**, *41*, 3389.

(13) Zaccheddu, M.; Filippi, C.; Buda, F. *J. Phys. Chem. A* **2008**, *112*, 1627.

(14) Quiñonero, D.; Frontera, A.; Escudero, D.; Costa, A.; Ballester, P.; Deyà, P. M. *Theor. Chem. Acc.* **2008**, DOI: 10.1007/s00214-008-0416-9.

(15) Mignon, P.; Loverix, S.; De Proft, F.; Geerlings, P. *J. Phys. Chem. A* **2004**, *108*, 6043.

(16) (a) Bader, R. F. W. *Chem. Rev.* **1991**, *91*, 893. (b) Bader, R. F. W. *Atoms in Molecules. A Quantum Theory*; Clarendon: Oxford, 1990.

(17) (a) Cheeseman, J. R.; Carrol, M. T.; Bader, R. F. W. *Chem. Phys. Lett.* **1998**, *143*, 450. (b) Koch, U.; Popelier, P. L. A. *J. Phys. Chem.* **1995**, *99*, 9794. (c) Cubero, E.; Orozco, M.; Luque, F. J. *J. Phys. Chem. A* **1999**, *103*, 315.

(18) Frisch, M. J.; Trucks, G. W.; Schlegel, H. B.; Scuseria, G. E.; Robb, M. A.; Cheeseman, J. R.; Montgomery, J. A., Jr.; Vreven, T.; Kudin, K. N.; Burant, J. C.; Millam, J. M.; Iyengar, S. S.; Tomasi, J.; Barone, V.; Mennucci, B.; Cossi, M.; Scalmani, G.; Rega, N.; Petersson, G. A.; Nakatsuji, H.; Hada, M.; Ehara, M.; Toyota, K.; Fukuda, R.; Hasegawa, J.; Ishida, M.; Nakajima, T.; Honda, Y.; Kitao, O.; Nakai, H.; Klene, M.; Li, X.; Knox, J. E.; Hratchian, H. P.; Cross, J. B.; Bakken, V.; Adamo, C.; Jaramillo, J.; Gomperts, R.; Stratmann, R. E.; Yazyev, O.; Austin, A. J.; Cammi, R.; Pomelli, C.; Ochterski, J. W.; Ayala, P. Y.; Morokuma, K.; Voth, G. A.; Salvador, P.; Dannenberg, J. J.; Zakrzewski, V. G.; Dapprich, S.; Daniels, A. D.; Strain, M. C.; Farkas, O.; Malick, D. K.; Rabuck, A. D.; Raghavachari, K.; Foresman, J. B.; Ortiz, J. V.; Cui, Q.; Baboul, A. G.; Clifford, S.; Cioslowski, J.; Stefanov, B. B.; Liu, G.; Liashenko, A.; Piskorz, P.; Komaromi, I.; Martin, R. L.; Fox, D. J.; Keith, T.; Al-Laham, M. A.; Peng, C. Y.; Nanayakkara, A.; Challacombe, M.; Gill, P. M. W.; Johnson, B.; Chen, W.; Wong, M. W.; Gonzalez, C.; Pople, J. A. *Gaussian 03*, revision C.02; Gaussian, Inc.: Wallingford, CT, 2004.

(19) Boys, S. B.; Bernardy, F. *Mol. Phys.* **1970**, *19*, 553.

(20) (a) Berryman, O. B.; Bryantsev, V. S.; Stay, D. P.; Johnson, D. W.; Hay, B. P. *J. Am. Chem. Soc.* **2007**, *129*, 48. (b) Maheswari, P. U.; Modec, B.; Pevec, A.; Kozlevcâr, B.; Massera, C. *Inorg. Chem.* **2006**, *45*, 6637. (c) Antonisse, M. M. G.; Snellink-Ruel, B. H. M.; Yigit, I.; Engbersen, J. F. J.; Reinhoudt, D. N. *J. Org. Chem.* **1997**, *62*, 9034.

(21) http://www.AIM2000.de.

(22) Luque, F. J.; Orozco, M. *J. Comput. Chem.* **1998**, *19*, 866.

(23) (a) Hernández, B.; Orozco, M.; Luque, F. J. *J. Comput.-Aided Mol. Des.* **1997**, *11*, 153. (b) Luque, F. J.; Orozco, M. *J. Chem. Soc., Perkin Trans. 2* **1993**, 683. (c) Quiñonero, D.; Frontera, A.; Garau, C.; Ballester, P.; Costa, A.; Deyà, P. M. *ChemPhysChem.* **2006**, *7*, 2487.

(24) Scrocco, E.; Tomasi, J. *Top. Curr. Chem.* **1973**, *42*, 95.

(25) Orozco, M.; Luque, F. J. *J. Comput. Chem.* **1993**, *14*, 587.

(26) Francl, M. M. *J. Phys. Chem.* **1985**, *89*, 428.

(27) (a) Frontera, A.; Quiñonero, D.; Garau, C.; Costa, A.; Ballester, P.; Deya, P. M. *J. Phys. Chem. A* **2006**, *110*, 9307. (b) Frontera, A.; Quiñonero, D.; Garau, C.; Costa, A.; Ballester, P.; Deya, P. M. *J. Phys. Chem. A* **2006**, *110*, 5144. (c) Quiñonero, D.; Frontera, A.; Garau, C.; Ballester, P.; Costa, A.; Deyà, P. M.; Pichierri, F. *Chem. Phys. Lett.* **2005**, *408*, 59. (d) Frontera, A.; Quiñonero, D.; Garau, C.; Ballester, P.; Costa, A.; Deyà, P. M.; Pichierri, F. *Chem. Phys. Lett.* **2005**, *417*, 372.

(28) Allen, F. H. *Acta Crystallogr.* **2002**, *B58*, 380.

(29) Nangia, A.; Biradha, K.; Desiraju, G. R. *J. Chem. Soc., Perkin Trans. 2* **1996**, 943.

(30) Bourne, S. A.; Corin, K. C.; Nassimbeni, L. R.; Toda, F. *Cryst. Growth Des.* **2005**, *5*, 372.

(31) Hatano, B.; Alkawa, A.; Tagaya, H.; Takahashi, H. *Chem. Lett.* **2004**, *33*, 1276.

JP802370S